Separation Science and Technology
Publication details, including instructions for authors and subscription information:
http://www.informaworld.com/smpp/title~content=t713708471

Fast Adsorption of Crystal Violet on Polyacrylic Acid-Bound Magnetic Nanoparticles

Min-Hung Liao[a]; Kun-Yang Wu[a]; Dong-Hwang Chen[a]
[a] Department of Chemical Engineering, National Cheng Kung University, Tainan, Taiwan, R.O.C.

To cite this Article Liao, Min-Hung , Wu, Kun-Yang and Chen, Dong-Hwang(2005) 'Fast Adsorption of Crystal Violet on Polyacrylic Acid-Bound Magnetic Nanoparticles', Separation Science and Technology, 39: 7, 1563 — 1575
To link to this Article: DOI: 10.1081/SS-120030802
URL: http://dx.doi.org/10.1081/SS-120030802

SEPARATION SCIENCE AND TECHNOLOGY
Vol. 39, No. 7, pp. 1563–1575, 2004

Fast Adsorption of Crystal Violet on Polyacrylic Acid-Bound Magnetic Nanoparticles

Min-Hung Liao, Kun-Yang Wu, and Dong-Hwang Chen*

Department of Chemical Engineering, National Cheng Kung University,
Tainan, Taiwan, R.O.C.

ABSTRACT

The adsorption of crystal violet from an aqueous solution by polyacrylic acid-bound magnetic nanoparticles was studied. It was shown that the magnetic nano-adsorbent was quite efficient for the adsorption/desorption of crystal violet. In the aqueous solution of crystal violet at 25°C, the adsorption behavior followed the Langmuir adsorption isotherm with a maximum adsorption amount of $116\,\mathrm{mg\,g^{-1}}$ and a Langmuir adsorption equilibrium constant of $0.005\,\mathrm{L\,mg^{-1}}$. In the methanol solution of acetic acid (1.0–8.0%), desorption of crystal violet increased up to 100% with increasing the acetic acid concentration. The reusability of magnetic nano-adsorbent and the effects of temperature, pH, and phosphate on the adsorption of crystal violet were also investigated.

---

*Correspondence: Dong-Hwang Chen, Department of Chemical Engineering, National Cheng Kung University, Tainan, Taiwan 701, R.O.C.; Fax: 886-6-2344496; E-mail: chendh@mail.ncku.edu.tw.

DOI: 10.1081/SS-120030802 0149-6395 (Print); 1520-5754 (Online)

www.dekker.com

Additionally, it was very noteworthy that the adsorption/desorption rate of crystal violet was quite fast (required time < 1 min) due to the absence of pore-diffusion resistance. The developed magnetic nano-adsorbent will be useful in the removal of cationic dyes from wastewater.

Key Words: Adsorption; Polyacrylic acid; Crystal violet; Magnetic nanoparticles; Nano.

INTRODUCTION

Effluents from the textile industries are important sources of water pollution, because dyes in wastewater undergo chemical as well as biological changes, consume dissolved oxygen, and destroy aquatic life. Moreover, some dyes and their degradation products may be carcinogens and toxic.[1,2] Therefore, it is necessary to treat textile effluents prior to their discharge into the receiving water.

Adsorption is a conventional but efficient technique to remove dyes from aqueous solutions. Many kinds of adsorbents for various applications have been commercialized or are developing.[3,4] In general, these adsorbents are highly porous particles in order to ensure adequate surface area for adsorption. However, the existence of intraparticle diffusion may lead to decreases in the adsorption rate and available capacity, particularly for macromolecules. Therefore, to develop an adsorbent with large surface area and small diffusion resistance has significant importance in practical use.[5]

Magnetic nanoparticles have great applications in the fields of high-density data storage, ferrofluids, magnetic resonance imaging, wastewater treatment, bioseparation, and biomedicine.[6–13] They meet the above requirements and can be easily recovered or manipulated with an external magnetic field. Numerous types of magnetic nanoparticles for various applications could be tailored by using functionalized natural or synthetic polymers to impart surface reactivity.[6,10]

Recently, we developed a novel magnetic nano-adsorbent using iron oxide nanoparticles as cores and polyacrylic acid (PAA) as ionic exchange groups.[14] It possessed a high ion-exchange capacity and was quite effective for the enzyme recovery. In this work, the PAA-bound magnetic nanoparticles were further used for the removal of a basic dye, crystal violet. The structure of crystal violet is shown in Sch. 1. It is a cationic dye and also belongs to the group of triphenylmethane dyes. However, some triphenylmethane dyes were found to induce renal, hepatic, and lung tumors in mice.[13,15] Therefore, it is important to treat crystal violet in the environment. In order to obtain information on treating crystal violet from the industry, the influences of experimental conditions such as crystal violet concentration, pH, temperature, salts, and desorption solution were also investigated.

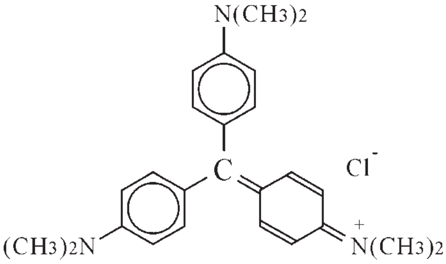

Scheme 1. Molecular structure of crystal violet.

EXPERIMENTAL

Materials

Polyacrylic acid solution (25%, degree of polymerization = 2000–3000) and crystal violet were purchased from Showa Chemical Co. (Tokyo). Carbodiimide was supplied by Sigma Chemical Co. (St. Louis, MO). Ferric chloride 6-hydrate and ferrous chloride tetrahydrate were the products of JT Baker (Phillipsburg) and Fluka (Buchs), respectively. Ammonium hydroxide (29.6%) was supplied by TEDIA (Fairfield). The water used throughout this work was the reagent-grade water produced by Milli-Q SP ultra-pure-water purification system of Nihon Millipore Ltd., Tokyo. All other chemicals were guaranteed or analytic grade reagents commercially available and used without further purification.

Preparation of PAA-Bound Iron Oxide Magnetic Nanoparticles

PAA-bound magnetic nanoparticles were prepared according to our previous works.[16] Iron oxide nanoparticles were prepared by coprecipitating Fe^{2+} and Fe^{3+} ions by ammonia solution and treating under hydrothermal conditions. The ferric and ferrous chlorides (molar ratio 2 : 1) were dissolved in water at a concentration of 0.3 M iron ions. Chemical precipitation was achieved at 25°C under vigorous stirring by adding NH_4OH solution (29.6%). During the reaction process, the pH was maintained at about 10. The precipitates were heated at 80°C for 30 min, then washed several times with deionized water and ethanol, and finally dried in a vacuum oven at 70°C.

For the binding of PAA, 100 mg of iron oxide nanoparticles were first added to 2 mL of buffer A (0.003 M phosphate, pH 6). Then, the reaction mixture was sonicated for 10 min after adding 0.5 mL of carbodiimide solution (0.025 g mL^{-1} in buffer A). Finally, 2.5 mL of PAA solution (60 mg mL^{-1} in buffer A) was added and the reaction mixture was sonicated for 30 min. The binding process was carried out at a constant temperature of 4°C. The PAA-bound iron oxide nanoparticles were recovered from the reaction mixture by placing the bottle on a permanent magnet with a surface magnetization of 6000 G. They settled within 1–2 min and then were washed with deionized water.

Characterization

The size of iron oxide nanoparticles was observed by transmission electron microscopy (TEM) using a JEOL Model JEM-1200EX at 80 kV. The magnetic measurement was done using a superconducting quantum interference device (SQUID) magnetometer (MPMS7, Quantum Design). The amount of PAA-bound on iron oxide nanoparticles was estimated by the percentage weight losses from the thermogravimetric analysis (TGA) done on the dried magnetic nanoparticles in air with a heating rate of 10°C min^{-1} on the Shimadzu TA-50WSI TGA. The ionic exchange capacity of PAA-bound iron oxide magnetic nanoparticles was determined as follows. First, 112 mg of nanoparticles were incubated in 5 mL of 1.0 M NaCl. The preliminary experiment revealed the adsorption process reached equilibrium after mixing by vortex for about 1 min; the nanoparticles were recovered magnetically after several minutes and then rinsed with water. Second, the nanoparticles were added to 5 mL of HNO_3 solution (pH 3) to release the Na^+ ions. After mixing by vortex for several minutes, the mixture was separated magnetically and the supernatant was used to determine the concentration of Na^+ ions by inductively coupled plasma atomic emission spectrometry (Jobin Yvon PA Norama).

Adsorption and Desorption Studies

The adsorption of crystal violet on the magnetic nano-adsorbent was investigated in deionized water at 25–65°C. For the studies of pH and salt effects, the adsorption of crystal violet was investigated in 0–0.5 M phosphate buffer (pH 2–9) at 25°C. The solution pH was measured using a pH meter (AUT-211, TOA). The pH value of phosphate buffer was adjusted by mixing the appropriate volume of sodium dihydrogenphosphate, disodium phosphate, or phosphoric acid solutions with the same phosphate concentration. In general, 112 mg of magnetic nano-adsorbent was added to 5 mL of crystal violet solution (100–6300 mg L^{-1}). After mixing by vortex for 1 min, the magnetic nano-adsorbents could be completely removed magnetically from the crystal violet solution using a permanent magnet with a surface magnetization of 6000 G. The amount of crystal violet adsorbed on the magnetic nano-adsorbent was estimated from the concentration change of crystal violet in solution after adsorption by the colorimetric method at 590 nm.[13] The blank test indicated that the adsorption of crystal violet to the glassware was negligible in this work because the adsorption time was only several minutes. From the established calibration curve, the extinction coefficient was found to be 0.1753 L mg^{-1} cm^{-1} within the concentration range of 0–10 mg L^{-1}. Desorption of crystal violet was studied by putting the removed magnetic nanoparticles into the methanol solution containing 1.0%–8.0% acetic acid. After mixing for several minutes and removing the magnetic nano-adsorbent, the concentration of crystal violet in liquid solution was measured to estimate the amount of crystal violet desorbed.

Reusability Assay

The reusability of magnetic nano-adsorbent was examined by conducting the adsorption/desorption measurement of magnetic nano-adsorbent at 25°C as stated above at a time interval of 50 min. After each adsorption/desorption measurement, magnetic nano-adsorbent was washed several times with methanol and deionized water.

RESULTS AND DISCUSSION

Characteristics of PAA-Bound Magnetic Nanoparticles

From the TEM analysis, the resultant PAA-bound iron oxide nanoparticles were found to be very fine. Their mean diameter was 12 nm. The magnetic measurement indicated that they were superparamagnetic with a saturation magnetization of 62 emu g^{-1} at 25°C. The TGA curve for the PAA-bound iron oxide nanoparticles showed a sharp weight loss of about 10.7% around 260°C due to the burning of PAA, and remained unchanged from 260°C to 400°C because only iron oxide existed within the temperature range. Thus, the weight ratio of bound PAA to Fe_3O_4 could be calculated to be 0.12. Using the density of Fe_3O_4 (5.18 g mL^{-1}) and the average molecular weight of PAA (180,000), it was estimated that on average two PAA molecules were bound to each Fe_3O_4 nanoparticle. The feasibility of PAA-bound magnetic nanoparticles was investigated in 1.0 M NaCl. It was found that the ionic exchange capacity of PAA-bound magnetic nanoparticles was

1.64 meq g^{-1}, much higher than those of the commercial ionic exchange resins. The preliminary experiment revealed that the ionic exchange capacity of naked magnetic nanoparticles for the adsorption of Na^+ ions was negligible (< 0.02 meq g^{-1}) compared to that of PAA-bound ones.

Adsorption and Desorption of Crystal Violet

Figure 1 shows the equilibrium isotherm for the adsorption of crystal violet on magnetic nano-adsorbent (22.4 mg mL^{-1}) in deionized water at 25°C. The adsorption behavior could be described with the Langmuir adsorption equation as[7]

$$\frac{C}{q} = \frac{1}{Kq_m} + \frac{C}{q_m} \tag{1}$$

where q is the adsorbed crystal violet concentration (mg g^{-1}), C is the equilibrium crystal violet concentration in solution (mg L^{-1}), q_m is the maximum amount of adsorbed crystal violet per gram of adsorbent (mg g^{-1}), and K is the Langmuir adsorption equilibrium constant (L mg^{-1}). As shown in the inset in Fig. 1, the plot of C/q vs. C yielded a straight line. From the slope and intercept, the values of q_m and K might be estimated to be 116 mg g^{-1} and 0.005 L mg^{-1}, respectively.

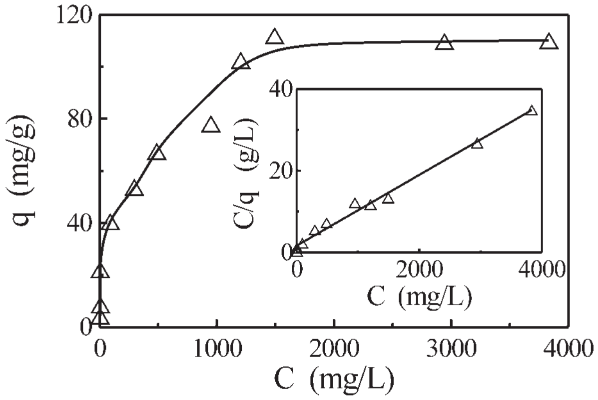

Figure 1. Equilibrium isotherm for the adsorption of crystal violet in the deionized water at 25°C. The inset illustrates the linear dependence of C/q on C. [Magnetic nano-adsorbent] = 22.4 mg mL^{-1} and [Crystal violet]$_{added}$ = 100–6300 mg L^{-1}.

Marcel Dekker, Inc.
270 Madison Avenue, New York, New York 10016

The desorption of crystal violet can be achieved using a methanol solution of acetic acid.[7,13] As shown in Fig. 2, the percentage of crystal violet desorbed increased with increasing the content of acetic acid. When the content of acetic acid in methanol solution was increased up to 6 vol%, crystal violet could be completely desorbed.

The adsorption and desorption measurements were conducted for the periods of 1 min to 24 hr, and it was notable that both equilibriums were reached within 1 min. Such fast adsorption and desorption rates could be referred to the absence of internal diffusion resistance. Accordingly, although the capacity was slightly lower than those of some natural and synthetic zeolites,[17] the magnetic nano-adsorbent with quite high adsorption capacity and fast adsorption rate owing to high specific surface area and none of internal diffusion resistance was useful for the separation of large molecules.

Effect of Temperature

The effect of temperature on the adsorption of crystal violet (4000 mg L^{-1}) on magnetic nano-adsorbent (22.4 mg mL^{-1}) was investigated in deionized water at 25–65°C. As shown in Fig. 3, the amount of crystal violet adsorbed decreased with increasing temperature. They might be due to the fact that the electrostatic interaction between crystal violet and PAA was lower at a higher temperature. The plot of $\ln(q/C)$ vs. $1/T$ was indicated in the inset in Fig. 3. From the slope $(-\Delta H/R)$, the change of enthalpy (ΔH) at 25–65°C could be determined to be -24.5 kJ mol^{-1}.[18]

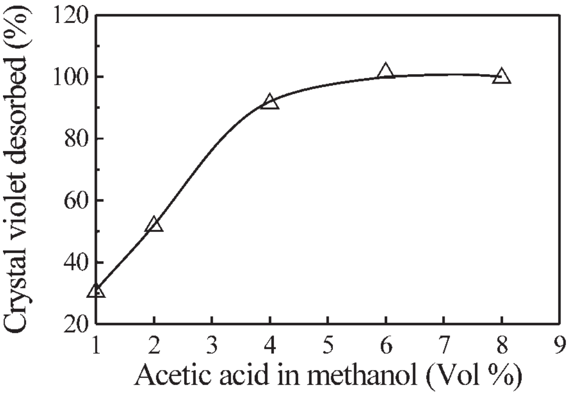

Figure 2. Effect of acetic acid content on the percentage of crystal violet desorbed in the methanol solution containing acetic acid. [Magnetic nano-adsorbent] = 22.4 mg mL^{-1} and [Crystal violet]$_{\text{added}}$ = 2000 mg L^{-1}.

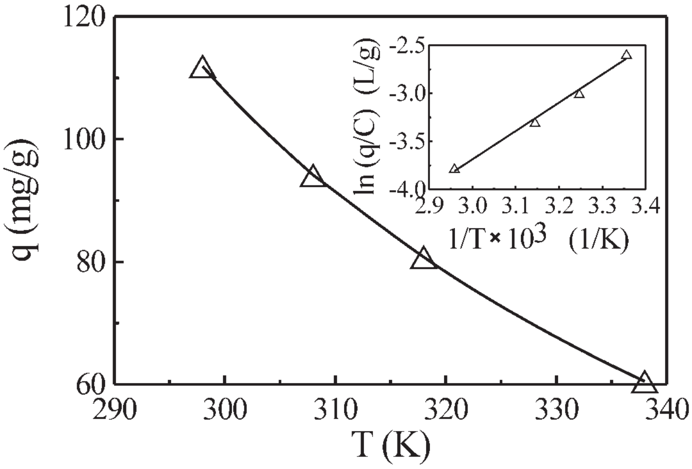

Figure 3. Effect of temperature on the amount of crystal violet adsorbed in the deionized water. The inset is the plot of $\ln(q/C)$ against $1/T$. [Magnetic nano-adsorbent] = 22.4 mg mL^{-1} and $[\text{Crystal violet}]_{\text{added}} = 4000\,\mathrm{mg\,L}^{-1}$.

Effect of pH

The adsorption of crystal violet by magnetic nano-adsorbents in 0.05 M phosphate buffer at pH 2–7, 2000 mg crystal violet L^{-1}, and 25°C is illustrated in Fig. 4. It was found that the adsorption amount of crystal violet was not significantly affected by solution pH at pH 4–9 due to its ionic structure.[19] The pK value for the protonation of crystal violet is about 1.[20] So, crystal violet is positively charged above pH 1. The adsorption amount of crystal violet slightly decreased with decreasing the solution pH at pH 2–4. This could be referred to as the protonation of carbonyl groups, which became significant at low pH.

Effect of Phosphate

The effect of phosphate concentration on the adsorption of crystal violet on magnetic nano-adsorbent at pH 6, 3000 mg crystal violet L^{-1}, and 25°C was illustrated in Fig. 5. It revealed that, with increasing phosphate concentration, the adsorption amount of crystal violet increased first and then approached a constant value. The maximum increment was about 32 mg g^{-1}. However, if phosphate was replaced by KCl, the adsorption amount of crystal

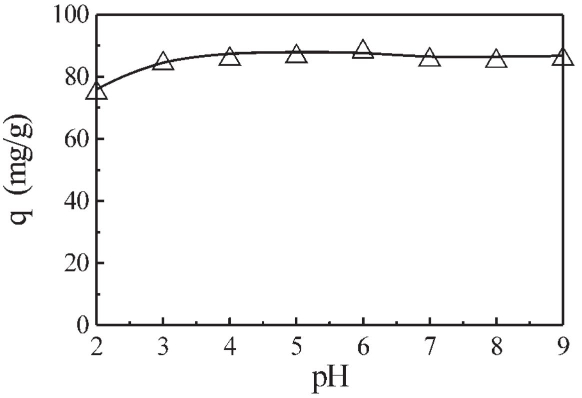

Figure 4. Effect of pH on the amount of crystal violet adsorbed in the 0.05 M phosphate buffer at 25°C. [Magnetic nano-adsorbent] = 22.4 mg mL^{-1} and [Crystal violet]$_{added}$ = 2000 mg L^{-1}.

violet had no significant changes. Thus, the phosphate effect should not be referred to the ionic strength effect.

To further investigate the phosphate effect, the adsorption of crystal violet by the naked magnetic nanoparticles (i.e., PAA was not bound) was carried out. The result was also indicated in Fig. 5. It was obvious that the naked

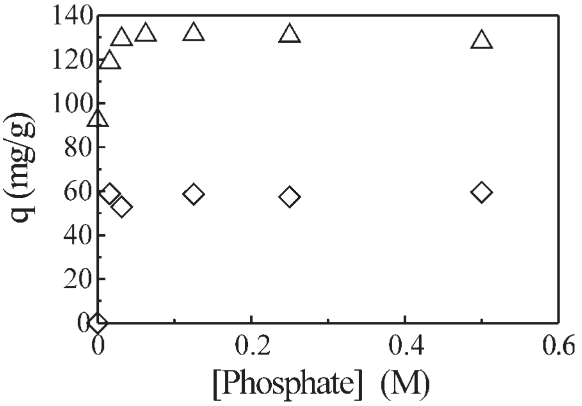

Figure 5. Effect of phosphate concentration on the adsorption amount of crystal violet on PAA-bound (△) and naked (◇) magnetic nanoparticles at pH 6 and 25°C. [PAA-bound magnetic nanoparticles] = 22.4 mg mL^{-1}, [Naked magnetic nanoparticles] = 20.0 mg mL^{-1}, and [Crystal violet]$_{added}$ = 3000 mg L^{-1}.

magnetic nanoparticles did not adsorbed crystal violet in water. That is, in the absence of phosphate, the adsorption of crystal violet by the PAA-bound magnetic nanoparticles was indeed attributed to the electrostatic attraction between the negatively charged PAA molecules and the positively charged crystal violet molecules. However, in the presence of phosphate, crystal violet could be adsorbed significantly on the naked magnetic nanoparticles, and the adsorption amount almost remained at about 58 mg g^{-1} in the examined phosphate concentration range. This implied the presence of a saturated adsorption amount. Also, the increased adsorption amount of crystal violet on the PAA-bound magnetic nanoparticles in the presence of phosphate might be contributed from the Fe_3O_4 cores instead of the PAA molecules. As for why the maximum increment in the adsorption amount of crystal violet by the PAA-bound magnetic nanoparticles in the presence of phosphate was smaller than that using the naked magnetic nanoparticles, it might be attributed to the bound PAA molecules, which occupied partial surface area of Fe_3O_4 cores and generated a negatively charged barrier to hinder the diffusion and adsorption of phosphate. Imamura et al.[21] studied the adsorption of methylene blue (another cationic dye) on the stainless steel surface, and also found that the presence of phosphate could increase the adsorption amount. They suggested that a monolayer of phosphate ions (PO_4^{3-}, HPO_4^{2-}, and $H_2PO_4^-$) associated with $-OH_2^+$ or $-O^-$ groups (depending on the solution pH) might be formed on the stainless steel surface. Their finding was quite similar to ours. Therefore, in this work, it could be suggested that the presence of phosphate might result in the formation of a phosphate monolayer on the surface of Fe_3O_4 nanoparticles, which further led to the adsorption of crystal violet via the ion–ion interaction with phosphate ions.

Reusability of Nano-adsorbent

The reusability of the nano-adsorbent is important in practical application. According to Fig. 6, the adsorption capacity of magnetic nano-adsorbent had no significant loss after being reused seven times. This revealed the resultant magnetic nano-adsorbent had excellent reusability. In addition, also this revealed that PAA did not peel off the Fe_3O_4 nanoparticles. This could be attributed to the fact that PAA was covalently bound to Fe_3O_4 nanoparticles.

CONCLUSIONS

The developed magnetic nano-adsorbent possesses higher ionic exchange capacity and exhibited fast adsorption and desorption rates for crystal violet.

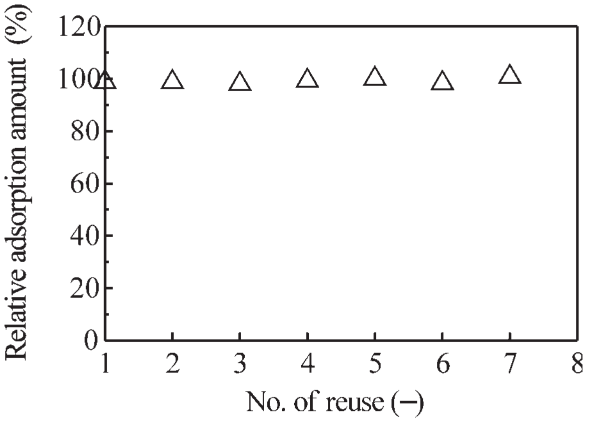

Figure 6. Relative adsorption amount of crystal violet on magnetic nano-adsorbent in the deionized water at 25°C. [Magnetic nano-adsorbent] $= 22.4\,\mathrm{mg\,mL^{-1}}$ and [Crystal violet]$_{\mathrm{added}} = 1000\,\mathrm{mg\,L^{-1}}$.

The adsorption behavior could be described by Langmuir isotherm, and the adsorbed crystal violet could be fully desorbed using the acetic acid-containing methanol solution at the appropriate condition. Both the adsorption and desorption of crystal violet reached equilibrium within 1 min due to internal diffusion resistance. This work should be helpful for the treatment of dye wastewater.

ACKNOWLEDGMENTS

This work was performed under the auspices of the National Science Council of the Republic of China, under contract number NSC90-2214-E006-009, for which the authors wish to express their thanks.

REFERENCES

1. Zollinger, H. *Color Chemistry*; VCH: New York, 1991.
2. Karadağ, E.; Üzüm, Ö.B.; Saraydin, D. Swelling equilibria and dye adsorption studies of chemically crosslinked superabsorbent acrylamide/maleic acid hydrogels. Eur. Polym. J. **2002**, *38*, 2133–2141.
3. McKay, G. *Use of Adsorbents for the Removal of Pollutants from Wastewaters*; CRC Press: Boca Raton, 1995.

4. Naim, M.M.; EI Abd, Y.M. Removal and recovery of dyestuffs from dyeing wastewaters. Sep. Purif. Methods **2002**, *31*, 171–228.
5. Dabrowski, A.; Bülow, M.; Podkościelny, P. Adsorption against pollution: current state and perspectives. In *Adsorption and Nanostructures*; Dekany, I., Ed.; Springer–Verlag: Heidelberg, 2002; 70–75.
6. Pieters, B.R.; Williams, R.A.; Webb, C. Magnetic carrier technology. In *Colloid and Surface Engineering: Applications in the Process Industries*; Williams, R.A., Ed.; Butterworth-Heinemann: Oxford, 1992; 248–286.
7. Šafařík, I. Removal of organic polycyclic compounds from water solutions with a magnetic chitosan based sorbent bearing copper phthalocyanine dye. Wat. Res. **1995**, *29*, 101–105.
8. Häfeli, U.; Schütt, W.; Teller, J.; Zborowski, M. *Scientific and Clinical Applications of Magnetic Carriers*; Plenum Press: New York, 1997.
9. Schütt, W.; Grüttner, C.; Häfeli, U.; Zborowski, M.; Teller, J.; Putzar, H.; Schümichen, C. Applications of magnetic targeting in diagnosis and therapy —possibilities and limitations: a mini-review. Hybridoma **1997**, *16*, 109–117.
10. Xu, Z.; Liu, Q.; Finch, J.A. Engineering of nanosize superparamagnetic particles for use in magnetic carrier technology. In *Surfaces of Nanoparticles and Porous Materials*; Schwarz, J.A., Contescu, C.I., Eds.; Marcel Dekker: New York, 1999; 31–50.
11. Denizli, A.; Say, R. Preparation of magnetic dye affinity adsorbent and its use in the removal of aluminium ions. J. Biomater. Sci. Pol. Edn. **2001**, *12*, 1059–1073.
12. Suber, L.; Foglia, S.; Ingo, G.M.; Boukos, N. Synthesis, and structural and morphological characterization of iron oxide–ion-exchange resin and cellulose nanocomposites. Appl. Organometal. Chem. **2001**, *15*, 414–420.
13. Šafařík, I.; Šafaříková, M. Detection of low concentrations of malachite green and crystal violet in water. Wat. Res. **2002**, *36*, 196–200.
14. Liao, M.H.; Chen, D.H. Preparation and characterization of a novel magnetic nano-adsorbent. J. Mater. Chem. **2002**, *12*, 3654–3659.
15. Rushing, L.G.; Hansen, E.B. Confirmation of malachite green, gentian violet and their leuco analogs in catfish and trout tissue by high-performance liquid chromatography utilizing electrochemistry with ultraviolet-visible diode array detection and fluorescence detection. J. Chromatogr. B **1997**, *700*, 223–231.
16. Chen, D.H.; Liao, M.H. Preparation and characterization of YADH-bound magnetic nanoparticles. J. Mol. Catal. B-Enzymatic **2002**, *16*, 283–291.
17. Harland, C.E. *Ion Exchange: Theory and Practice*; The Royal Society of Chemistry: Cambridge, 1994.

18. Bajpai, A.K. Adsorption of bovine serum albumin onto glass powder surfaces coated with polyvinyl alcohol. J. Appl. Polym. Sci. **2000**, *78*, 933–940.
19. Bohrer, D.; do Nascimento, P.C.; Seibert, E.; Carvalho, L.M. Polyethylene powder as an adsorbent for complexing dyes: influence of dye structure, solvent, pH, and ionic strength. Sep. Sci. Technol. **2002**, *37*, 2183–2199.
20. Hoppe, R.; Alberti, G.; Costantino, U.; Dionigi, C.; Schulz-Ekloff, G.; Vivani, R. Intercalation of dyes in layered zirconium phosphates. 1. Preparation and spectroscopic characterization of α-zirconium phosphate crystal violet compounds. Langmuir **1997**, *13*, 7252–7257.
21. Imamura, K.; Ikeda, E.; Nagayasu, T.; Sakiyama, T.; Nakanishi, K. Adsorption behavior of methylene blue and its congeners on a stainless steel surface. J. Colloid Interf. Sci. **2002**, *245*, 50–57.

Received August 2003
Accepted January 2004

Marcel Dekker, Inc.
270 Madison Avenue, New York, New York 10016

Downloaded At: 10:08 25 January 2011

Request Permission or Order Reprints Instantly!

Interested in copying and sharing this article? In most cases, U.S. Copyright Law requires that you get permission from the article's rightsholder before using copyrighted content.

All information and materials found in this article, including but not limited to text, trademarks, patents, logos, graphics and images (the "Materials"), are the copyrighted works and other forms of intellectual property of Marcel Dekker, Inc., or its licensors. All rights not expressly granted are reserved.

Get permission to lawfully reproduce and distribute the Materials or order reprints quickly and painlessly. Simply click on the "Request Permission/ Order Reprints" link below and follow the instructions. Visit the U.S. Copyright Office for information on Fair Use limitations of U.S. copyright law. Please refer to The Association of American Publishers' (AAP) website for guidelines on Fair Use in the Classroom.

The Materials are for your personal use only and cannot be reformatted, reposted, resold or distributed by electronic means or otherwise without permission from Marcel Dekker, Inc. Marcel Dekker, Inc. grants you the limited right to display the Materials only on your personal computer or personal wireless device, and to copy and download single copies of such Materials provided that any copyright, trademark or other notice appearing on such Materials is also retained by, displayed, copied or downloaded as part of the Materials and is not removed or obscured, and provided you do not edit, modify, alter or enhance the Materials. Please refer to our Website User Agreement for more details.

Request Permission/Order Reprints

Reprints of this article can also be ordered at

http://www.dekker.com/servlet/product/DOI/101081SS120030802